Supplemental materials of

Mechanistic description of Lead sorption onto nanoplastics

Florent Blancho[1], Mélanie Davranche[1], Adrien Léon[1], Rémi Marsac[1], Stéphanie Reynauld[2], Bruno Grassl[2], and Julien Gigault[1,3*]

[1] Univ Rennes, CNRS, Géosciences Rennes – UMR 6118, F-35000 Rennes, France.

[2] IPREM, CNRS / Université de Pau et des Pays de L'Adour, F64000 Pau, France

[3] TAKUVIK laboratoy, UMI3376 CNRS / Université Laval, Québec, Canada

S1. Nanoplastic characterization

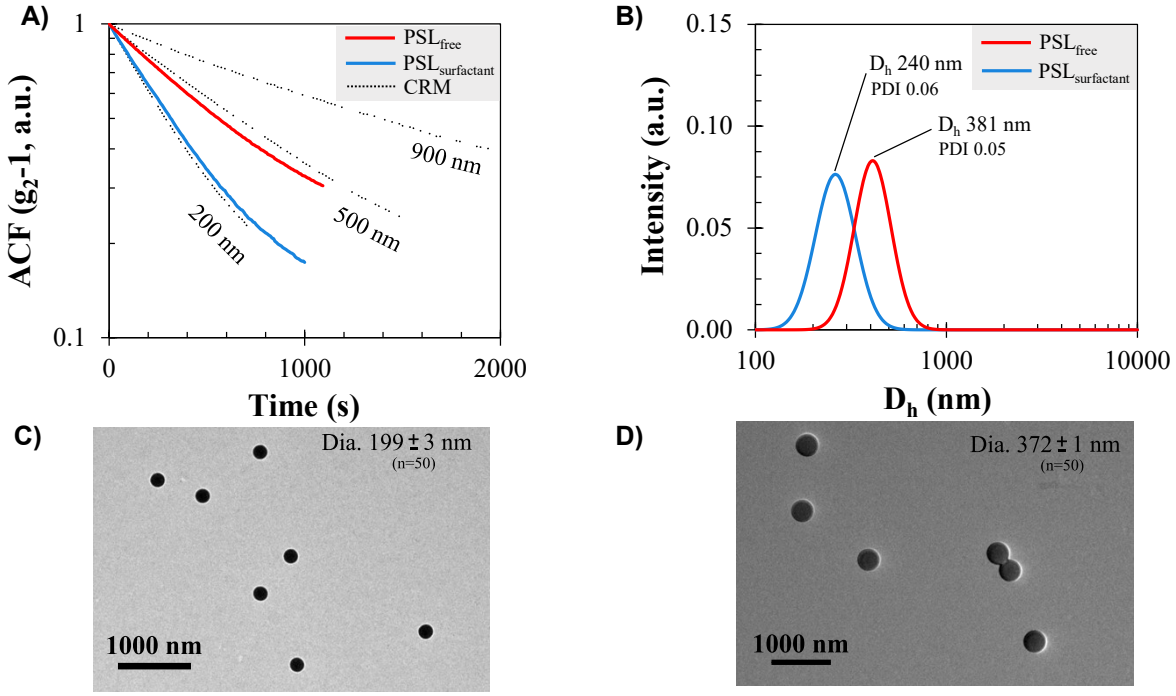

Fig. S1. NP size characterization. A) Log-transformed ACF of the e-NPs and m-NPs superimposed on CMRs standards (200, 500 and 900 nm). **B)** Population size distribution by intensity estimated with an ACF cumulant fit. **C-D)** TEM pictures of the $PSL_{surfactant}$ and PSL_{free}, respectively.

S2. Surface properties calculations

The determination of the protonable groups was performed as described by Spadini et al. (2018). Briefly, the proton released from the surface, H_s, was related to the pH of the solution (Eq. S1). The total surface site concentration, Hs_{tot}, was defined as the released H_s between pH 4 and 8.0 for the highest IS. Due to early site deprotonation, there is an initial charge at the surface of the NPs, denoted H_0. This H_0 is dependent on the ionic strength (IS) and was estimated by modelling calculations. This calculated H_0 was thus added to H_{surf}. The CO_2 diffusion during the titration was taken in account using the Hs_{tot} of the ultrapure water (blank).

$$[H^+] = [H_{init}] + [H_{base}] + [H_s] + [OH^-] \quad \text{(S1)}$$

Where $[H^+]$ = the free proton concentration, (M), $[H_{init}]$ = the concentration of acid added to fix the pH below pH 4 (M), $[H_{base}]$ = the concentration of base added during the titration (M), which is positive when a base is used and negative when an acid is used, $[H_s]$ = the concentration of the released H^+, the only unknown (M) and $[OH^-]$, the concentration of the H^+ released from the water auto-protolyze, at pH 7 (M).

The surface charge of the NPs was determined by performing a calculation using PHREEQC implemented by the SIT thermodynamic database.

The surface charge of the NPs was conceptualized as resulting from the ionizable surface groups (i.e. –OH, –COOH, etc.), overall represented as –SOH. Their dissociation was defined as conforming to the mass action law:

$$-SOH \Leftrightarrow -SO^- + H_s^+ \quad (2) \qquad K_{HL} = \frac{[-SO^-]\,[H_s^+]}{[-SOH]} \quad (S2)$$

A permanent charge due to a lattice defect was neglected for PSL, since it is latex, and is not taken into consideration for the e-NPs and m-NPs since they are amorphous. As a result, the total net particle charge, σ_P, is restricted to equation 3.

$$\sigma_P = \sigma_H + \sigma_{IS} \qquad (S3)$$

Where σ_H = the charge involved by the association/dissociation of H^+ on the ionizable groups and σ_{IS} = the charge of inner sphere complex.

The pKa were determined using a combination of geochemical (PHREEQC version 2) and extrapolation (PhreePlot) programs (Parkhurst and Appelo 1999, Kinniburgh and Cooper 2011) PhreePlot was designed in order to automatically fit experimental datasets using the speciation program PHREEQC. The binding parameters are optimized by a modified Marquardt-Levenberg procedure (Powell, 1965). The electrostatic energy term (i.e. coulombic interaction) was considered using a Diffuse Layer Model (DLM). As demonstrated by Blancho et al. (submitted), the sorption of trivalent cations was driven by –COOH for the two PSLs and the e-NPs models. As a result, for all NPs, the surface charge is explained and restricted to the presence of –COOH sites (Eq. 5).

$$-COOH^- + H_s^+ \Leftrightarrow -COOH \quad (S4) \qquad K_{-COOH} = \frac{[-COOH]}{[-COO^-] * [H^+]} * e^{\frac{\Psi_0}{kT}} \quad (S5)$$

Where Ψ_0 = the surface potential energy (J), k = Boltzman constant (J K^{-1}) and T = Temperature (K).

S3. Pb(II) Speciation relative to pH and saturation index calculation to predict precipitation

The Pb(II) speciation was simulated from pH 2 to 10 in order to define the predominant Pb(II) species over the geochemical conditions tested with PHREEQC (Parkhurst and Appelo, 1999) for a ionic strength set to 5 x 10^{-3} mol L^{-1}.

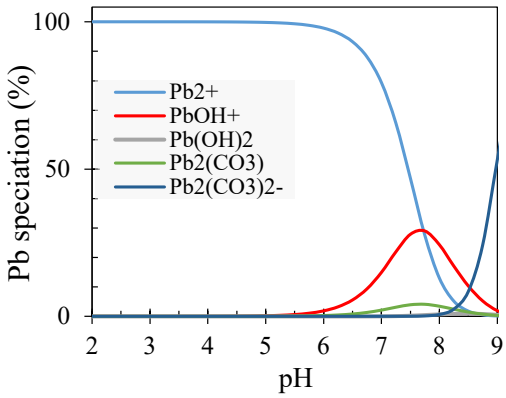

Fig. S2. Pb(II) speciation. Pb(II) hydrolysis species relative to pH.

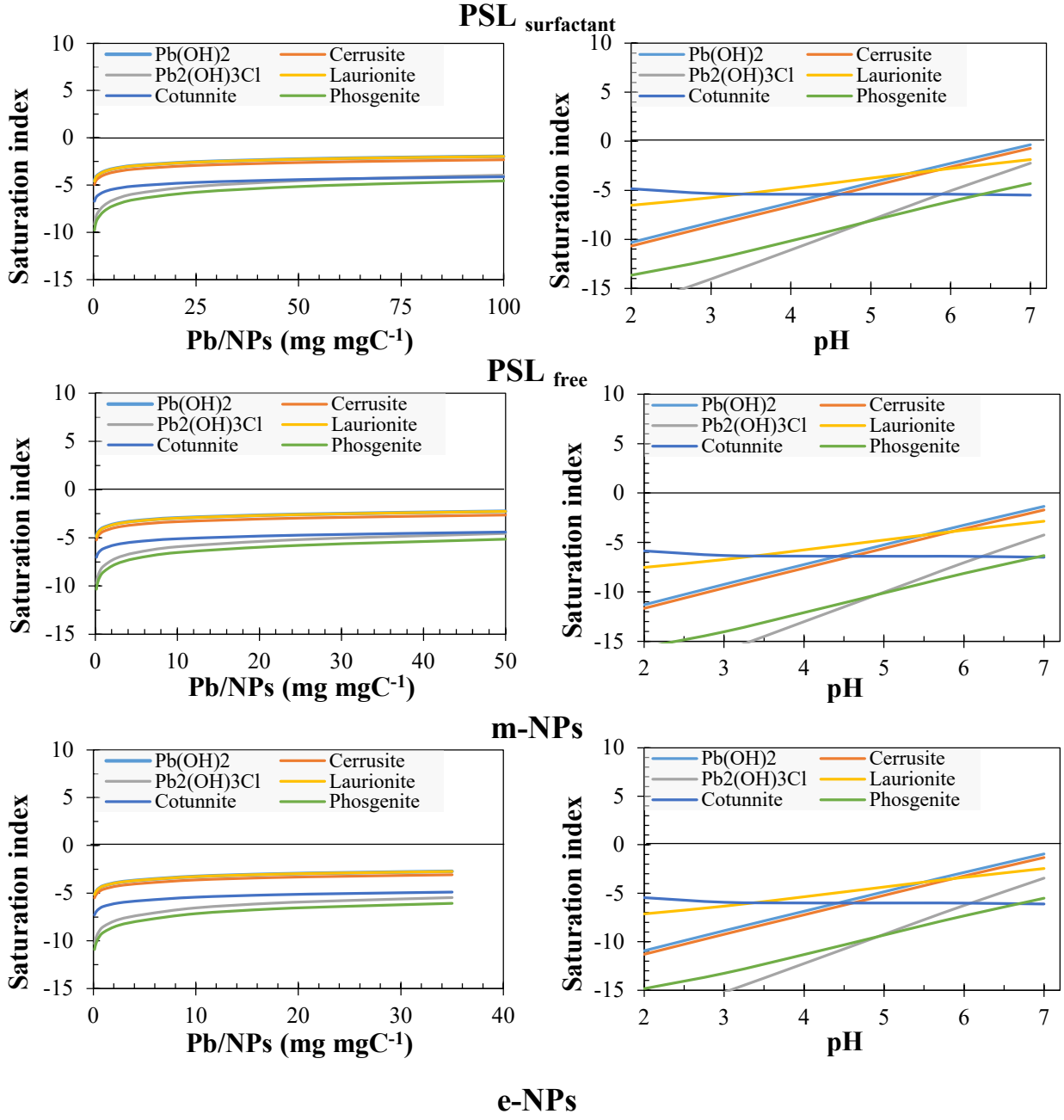

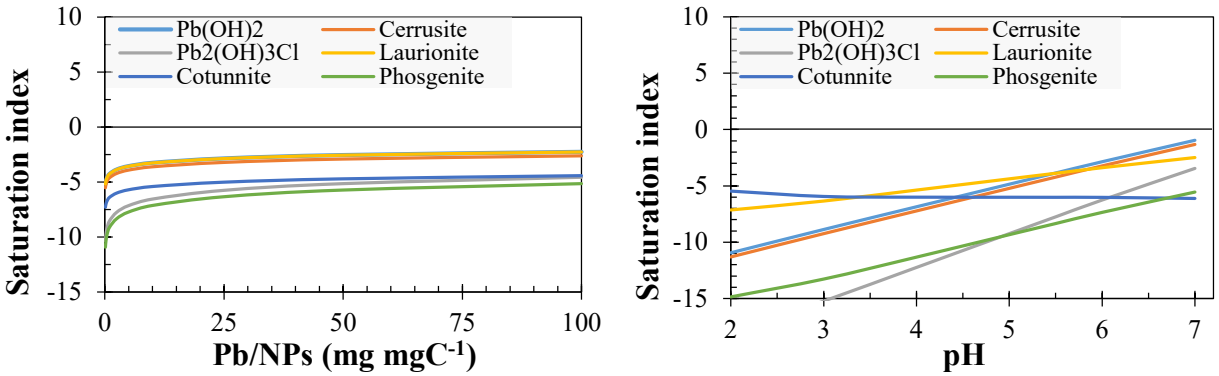

Fig. S3. Saturation indices of Pb-based solid phases. Saturation indices of the main Pb-based solid phases calculated at experimental conditions used for isotherm (left) and pH edge (right) adsorptions using PhreeQC with the MINTEQA2 database. Note that a solid phases saturation index < 0 indicates unsuitable conditions for precipitation.

S4. Classical Langmuir isotherm against double Langmuir isotherm for e-NPs

Figure SI 3 compares the classical and double Langmuir isotherm models for e-NPS adsorption isotherm dataset. The classical Langmuir model failed to reproduce the adsorbed Pb concentrations at low Pb_{free} concentrations (Figure SI 3) by contrast with the double-Langmuir model. This result provided evidence of the formation of two complexes between Pb and the -COOH binding sites developed at the e-NPS surface.

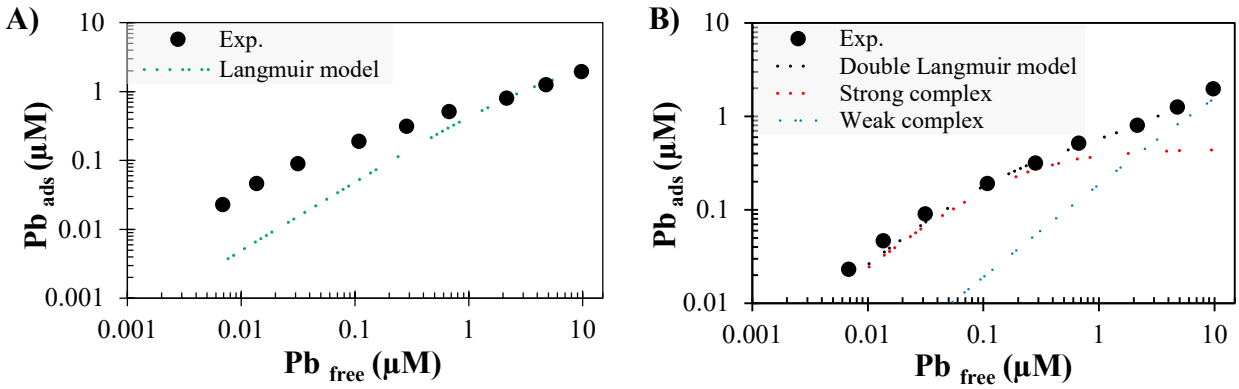

Fig. S4. Classical and double Langmuir model comparison. Comparison between **A)** the classical and **B)** the double Langmuir isotherm models for the Pb(II)-e-NPS adsorption isotherm.

Table S1. Langmuir and double-Langmuir parameters calculated for the adsorption of Pb(II) onto e-NPs.

Parameters	Classical Langmuir isotherm	Double Langmuir isotherm
Q (µM)	3.3	
log K	-0.83	
$RMSE_{langmuir}$	0.04	
Q_{weak} (µM)		7.06
log K_{weak}		-1.5
Q_{strong} (µM)		0.408
log K_{strong}		0.922
$RMSE_{double\text{-}Langmuir}$		0.0009

S5. Mechanistic model: mono- against bi-ligand hypothesis

In the Figure SI-3 are compared the calculated and experimental adsorption isotherms of Pb(II)-$PSL_{surfactant}$ and Pb(II)-m-NPs. The best fitting was chosen regarding the lowest RMSE value, the empirical modelling and the binding hypotheses suggested by Blancho et al. (2022) For the m-NPS, the calculated log K for the m-NPS-COO-Pb^{+} (mono-ligand binding hypotheses) was largely overestimated regarding the log K of the CH_3-COO-Pb+ from (Smith and Martell, 1989) avoiding its validation. By contrast, the log K calculated for the bi-ligand model, $(m\text{-}NPS\text{-}COO)_2$-Pb was in the range of that provided by (Smith and Martell, 1989), 4.95 against 4.77, respectively, allowing this binding hypothesis to be validated.

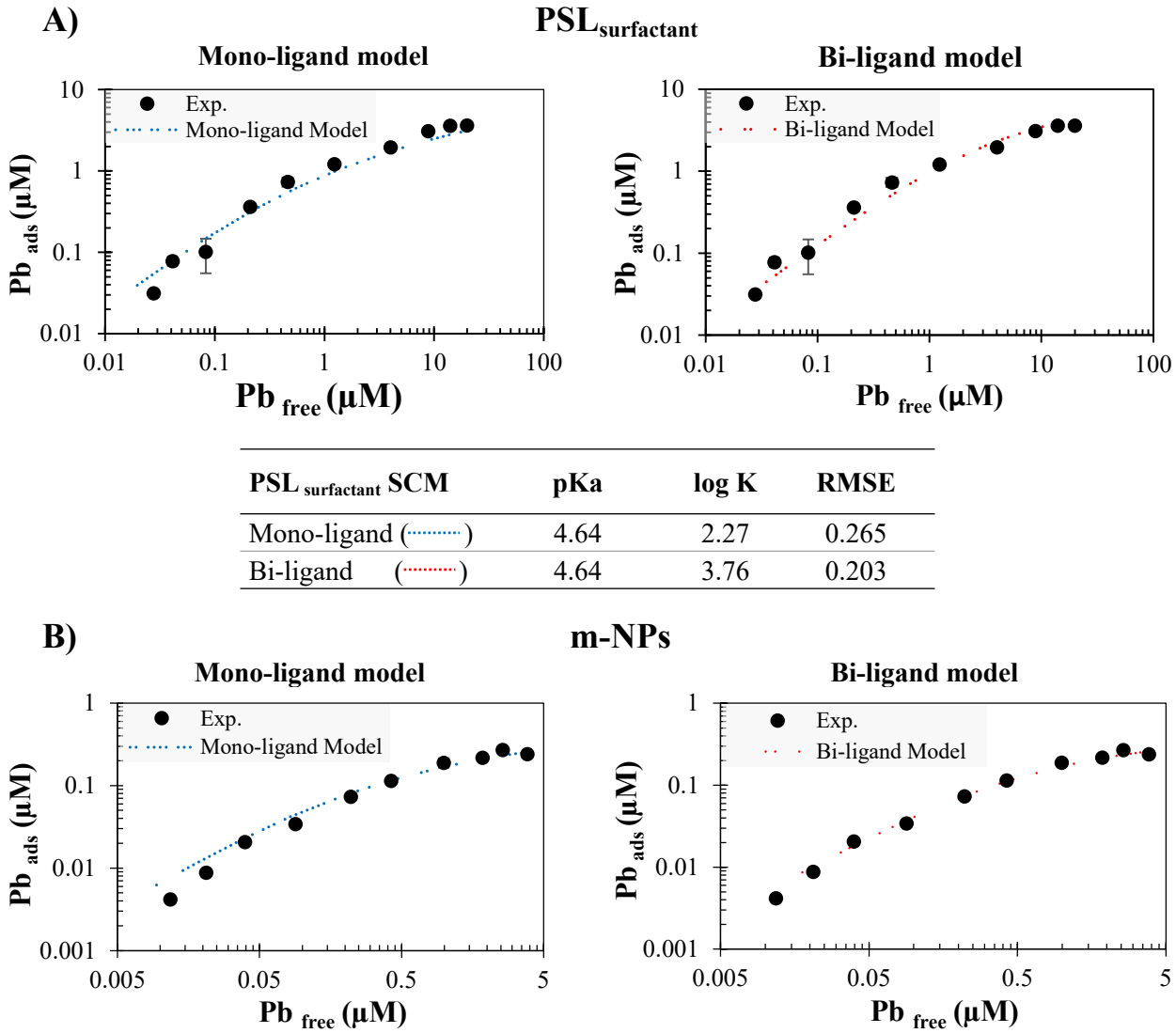

PSL surfactant SCM	pKa	log K	RMSE
Mono-ligand (·····)	4.64	2.27	0.265
Bi-ligand (·····)	4.64	3.76	0.203

m-NPs SCM	pKa	log K	RMSE
Mono-ligand (·····)	4.76	4.01 ± 0.07	0.018
Bi-ligand (·····)	4.76	4.94 ± 0.06	0.019

Fig. S5. Mono and bi-ligand Surface complex model comparison. A) Comparison between the mono-ligand and bi-ligands mechanistic models for the Pb(II)-$PSL_{surfactant}$ adsorption isotherm. **B)** Comparison between the mono-ligand and bi-ligands mechanistic models for the Pb(II)-m-NPs adsorption isotherm.

References

Kinniburgh, D., Cooper, D., 2011. PhreePlot: Creating graphical output with PHREEQC.

Parkhurst, D.L., Appelo, C.A.J., 1999. User's guide to PHREEQC (Version 2): A computer program for speciation, batch-reaction, one-dimensional transport, and inverse geochemical calculations. https://doi.org/10.3133/wri994259

Powell, M.J.D., 1965. A Method for Minimizing a Sum of Squares of Non-Linear Functions Without Calculating Derivatives. The Computer Journal 7, 303–307. https://doi.org/10.1093/comjnl/7.4.303

Smith, R.M., Martell, A.E., 1989. Carboxylic Acids, in: Smith, R.M., Martell, A.E. (Eds.), Critical Stability Constants: Second Supplement, Critical Stability Constants. Springer US, Boston, MA, pp. 299–359. https://doi.org/10.1007/978-1-4615-6764-6_12

Spadini, L., Navel, A., Martins, J.M.F., Vince, E., Lamy, I., 2018. Soil aggregates: a scale to investigate the densities of metal and proton reactive sites of organic matter and clay phases in soil. Eur J Soil Sci 69, 953–961. https://doi.org/10.1111/ejss.12695